Mineral Sequences in Precipitation/Dissolution Waves

A theory for flow through permeable media with equilibrium precipitation/dissolution interactions is rigorously established. The general solution in terms of waves, which represent the propagation of concentration changes is developed, and the detailed structure of a precipitation/dissolution wave in the presence of dissipation (diffusion and dispersion) is derived; this structure plays a vital role in the general solution. The solution is based on Riemann invariants and thus exhibits certain similarities to wave solutions of related problems in gas dynamics and chromatography. However, a discontinuity peculiar to the precipitation/dissolution problem prevents unification of these similar solutions into a single, more general theory.

S. L. Bryant, R. S. Schechter
Department of Chemical Engineering

L. W. Lake
Department of Petroleum Engineering
University of Texas
Austin, TX 78712

Introduction

An interesting and complex class of flows through permeable media is that in which the flowing fluid and the permeable medium interact chemically. Chemical interactions between an aqueous phase and a solid phase fall into two basic categories: exchange/adsorption interactions and precipitation/dissolution interactions. In an exchange/adsorption interaction, the solid phase binds some species from the fluid phase and releases others. In a precipitation/dissolution interaction, species in the fluid phase combine to form a solid phase precipitate and precipitates dissolve, returning their components to solution.

Regardless of the type, the most significant result of such fluid-solid interactions during flow is the formation and propagation of concentration changes through the medium. These concentration changes are called waves, in analogy with waves in fluid dynamics that carry changes in pressure, temperature, entropy, or other properties of the fluid (Courant and Friedrichs, 1948; Lighthill, 1978; Taniuti and Nishihara, 1983). The concentration changes carried by waves establish compositions in the medium quite different from the composition of the fluid injected into the medium and from the composition of the fluid and solids initially present in the medium.

The solution to a reactive flow problem describes the concentrations of species in the flowing and solid phases as functions of time and position in the medium. The broad variety of applications involving reactive flow through permeable media (e.g., enhanced oil recovery, groundwater contamination, mineral leaching) naturally leads to interest in a general solution that applies to as many individual problems as possible. Historically, flows with exchange/adsorption reactions have been vital for separation processes, so the theory for such flows is well developed (Wilson, 1940; DeVault, 1943; Glueckauf, 1946; Tondeur and Klein, 1967; Rhee at al., 1970, Helfferich and Klein, 1970). Only in recent years have the importance and applications of flows with precipitation/dissolution reactions been widely recognized. Fogler and Rege (1986) provide a summary of this work to date, and Cussler et al. (1983) present an example of precipitation/dissolution in diffusive systems.

Our work on reactions in viscously-dominated flow suggests that some relatively simple principles underlie flow with precipitation/dissolution reactions (Walsh, 1983; Walsh et al., 1984). A study of uranium ore leaching presented in that work found wave behavior strongly reminiscent of chromatographic waves, despite the great complexity of the applicable chemistry. Walsh et al. pointed out the importance of mineral sequences to the wave behavior. Based on a computer model, Walsh et al. also hypothesized that precipitation/dissolution waves must be coherent and suggested a downstream equilibrium condition. Using these principles the age and grade of uranium roll front deposits were successfully predicted from wave velocities and solid phase concentrations.

In this paper we establish for the first time the theory of flow with precipitation/dissolution reactions. This theory provides the general solution for such flows; it also verifies the simple laws posited by Walsh et al. and defines their limits. The precipitation/dissolution problem lacks a continuously differentiable isotherm relating the solid phase and flowing phase concentrations. This feature precludes the extension of theories for other sets of conservation equations, such as chromatography theory,

to the precipitation/dissolution problem. Some significant results of the theory are summarized below.

1. The solution of the precipitation/dissolution problem under Riemann conditions consists of constant-state sectors emanating from the origin of the time and distance axes.
2. The precipitation/dissolution waves that separate these sectors are coherent shocks.
3. The flowing phase concentrations must be calculated in the downstream direction from the injected conditions.
4. The solid concentrations must be calculated in the upstream direction from the initial conditions after the flowing phase concentrations have been determined.
5. Jump conditions obtained from the behavior of a precipitation/dissolution wave in the presence of dissipation (diffusion and dispersion) are necessary to determine the concentration changes across the wave in the absence of dissipation.
6. The downstream equilibrium condition provides the jump conditions for waves that completely dissolve exactly one solid.
7. The partial downstream equilibrium condition provides the jump conditions for waves that completely dissolve more than one solid.
8. The number of solids completely dissolved by a wave equals the number of discontinuities in the dissipation structure of the wave.
9. Finding the correct sequence of solid identities between the initial and injected conditions is necessary and sufficient for solving the general precipitation/dissolution problem.
10. A solution function derived from criteria for physical validity of sequences determines the correct sequence of identities.

Definition of the Precipitation/Dissolution Problem

Assumptions

We assume that a single incompressible phase of constant viscosity flows isothermally through a one-dimensional homogeneous permeable medium. For simplicity of presentation we assume an ideal flowing phase, so that activities of the species therein equal their concentrations. This assumption does not diminish the generality of the chemical description to be presented; it merely affects numerical calculations. In this paper we consider only reactions that attain thermodynamics equilibrium instantaneously at every position in the medium during flow (local equilibrium).

We also assume that the porosity ϕ of the permeable medium is constant during flow. Thus, reactive solids occupy a constant or negligibly small fraction of the bulk volume of the medium. Because ϕ is constant and the fluids incompressible, the superficial fluid velocity through the medium will be invariant with respect to position. Finally, the solid phase is incompressible and stationary, and solid particles do not migrate.

Chemical reactions

Suppose that the chemical species in a reactive flow are composed of I distinct chemical elements. Let J be the number of flowing phase species, and K the number of soluble solids possible. The soluble solids may either be present initially in the medium or may precipitate during flow. We describe all chemical reactions in this system in terms of I chemically independent flowing phase species (Smith and Missen, 1982; Stohs, 1986; Bryant et al., 1986). Within the flowing phase J–I reactions describe the formation of dependent species (products) from independent species (reactants):

$$\alpha_{ir}A_i' = A_r \quad r = I + 1, \ldots, J \tag{1}$$

(Symbols are defined in the Notations.) This description includes oxidation-reduction reactions that treat the electron as an independent species (Walsh et al., 1984). Equation 1 uses the convention that summation occurs over repeated subscript indices in multiplied terms.

The equilibrium expressions corresponding to Eq. 1 have the mass-action form:

$$K_r = C_r/C_i'^{\alpha_{ir}} \quad r = I + 1, \ldots, J \tag{2}$$

Multiplication occurs over repeated indices in subscripts of bases and exponents. Hence the righthand side of Eq. 2 is equivalent to $C_r/(\Pi_i C_i'^{\alpha_{ir}})$. The summation and multiplication conventions will be used throughout unless noted otherwise. The basis for all concentrations is the volume of fluid contained in a unit volume of the medium.

There are K heterogeneous reactions that describe the precipitation/dissolution of the soluble solids:

$$S_k = g_{ik}A_i' \quad k = 1, \ldots, K \tag{3}$$

The equilibrium expressions corresponding to these reactions are solubility product constraints. They have the form

$$K_k^{sp} = C_i'^{g_{ik}} \quad k = 1, \ldots, K \tag{4}$$

Equation 4 imposes no relation between the concentration of the solids and the concentrations in the flowing phase. In contrast, the equilibrium expressions for the other major class of fluid/solid interactions in reactive flow, i.e., adsorption/exchange reactions, in general are continuously differentiable relations between the flowing phase and solid concentrations. This peculiar feature of the solubility product constraint will be important in the theoretical development.

When the corresponding solid dissolves, a solubility product constraint becomes an inequality of the form

$$K_k^{sp} \geq C_i'^{g_{ik}} \tag{5}$$

This inequality prevents supersaturation of the flowing phase with respect to the dissolved solid in accordance with the assumption of local equilibrium. The number of inequalities like Eq. 5 that can constrain the flowing phase concentrations is unlimited. However, the number of equalities like Eq. 4 is limited by the number of independent species. The I independent species concentrations C_i' can satisfy at most $I - 1$ solubility products simultaneously with the electroneutrality condition in the flowing phase. Therefore at most $I - 1$ solids can occur at any position in the medium, so at all positions we have $I > K$.

Flow equations

There is a total of I mass balances, one for each independent species. Under our assumptions, the conservation of independent species A_i' takes the form of a parabolic partial differential equa-

tion:

$$\partial C_i^T/\partial t + \partial C_i/\partial x - (N_{Pe})^{-1}\partial^2 C_i/\partial x^2 = 0 \quad i = 1, \ldots, I \quad (6)$$

in dimensionless coordinates. C_i is the total flowing phase concentration of A_i' given by $h_{ij}C_j$, where C_j is the concentration of flowing phase species j. For independent species we have $C_j \equiv C_i'$ and $h_{ij} \equiv \delta_{ij}$ $(j, i \le I)$; for dependent species we have $C_j \equiv C_r$ and $h_{ij} \equiv \alpha_{ir}$ $(j, r = I + 1, \ldots, J)$. C_i^T is the total concentration of A_i' given by $C_i + g_{ik}\underline{C}_k$, where $\underline{C}_k$ is the concentration of solid S_k.

As implicitly indicated in Eq. 6, the diffusive/dispersive flux F_j of flowing phase species j is directly proportional to the flowing phase concentration gradient:

$$F_j = D_0 \partial C_j/\partial x \quad j = 1, \ldots, J \quad (7)$$

where D_0 is the coefficient of diffusion/dispersion. D_0 is assumed constant and equal for all species. For convenience we henceforth use the term dissipation to mean both diffusion and dispersion. In the limit of zero dissipation, the conservation equation, Eq. 6, becomes hyperbolic:

$$\partial C_i^T/\partial t + \partial C_i/\partial x = 0 \quad i = 1, \ldots, I \quad (8)$$

We will encounter curves in time-distance space at which one or more of the concentration derivatives in Eq. 8 do not exist. On these curves we apply an integral form of the mass balance. Letting $x_b(t)$ denote such a curve, an integral mass balance at the curve takes the form (in the absence of dissipation)

$$(1 - v_b)[C_i(x_b^-, t) - C_i(x_b^+, t)] - v_b[g_{ik}\underline{C}_k(x_b^-, t) - g_{ik}\underline{C}_k(x_b^+, t)] = 0 \quad (9)$$

where $v_b(t) = dx_b/dt$ is the slope of the curve. The superscripts + and − indicate the concentrations just downstream and upstream of the curve, respectively. Solving Eq. 9 for the velocity yields a more useful form of the integral mass balance:

$$v_b = (1 + \Delta g_{ik}\underline{C}_k/\Delta C_i)^{-1} \quad (10)$$

where $\Delta X = X(x_b^+) - X(x_b^-)$ is the jump in variable X across the curve.

The boundary conditions for Eq. 8 are the total independent species concentrations initially and at the inlet of the medium:

$$C_i^T(x, 0) = C_i^{T,init}(x) \quad i = 1, \ldots, I$$
$$C_i(0, t) = C_i^{inj}(t) \quad i = 1, \ldots, I \quad (11)$$

where superscripts *inj* and *init* indicate injected and initial states. Since solids are stationary, only flowing phase totals need to be specified at the inlet. In general, the injected conditions vary with time, and the initial conditions vary with distance. In this paper we consider only Riemann conditions, i.e., constant functions for $C_i^{T,init}$ and C_i^{inj}. A discussion of flow with precipitation/dissolution under non-Riemann conditions may be found elsewhere (Bryant, 1986).

Solution in Terms of Solid Identities

The solution of the precipitation/dissolution problem in the absence of dissipation, Eqs. 2, 4, 8, and 11, is most conveniently represented on time-distance diagrams, wherein lines and regions of constant composition are plotted on axes of dimensionless time and dimensionless distance. A boundary between regions of constant composition represents a wave propagating through the medium. The slope of such a boundary is the specific velocity of the wave (velocity as a fraction of the fluid velocity). We assume that the solution is unique, so it will suffice to exhibit *a* solution.

Intervals and regions of invariant solid identities

We introduce a covering postulate for flow with precipitation/dissolution reactions:

> At any time during flow the distance axis of the permeable medium is covered by the union of one or more intervals of invariant solid identities.

An interval of invariant solid identities (IISI) is a segment (x_1, x_2) of the permeable medium on which the concentration of every solid $(k = 1, \ldots, K)$ satisfies an identity invariance condition:

if $\underline{C}_k(x^*) = 0$ for some x^* on (x_1, x_2),
then $\underline{C}_k(x) = 0$ for all x on (x_1, x_2)

if $\underline{C}_k(x^*) > 0$ for some x^* on (x_1, x_2),
then $\underline{C}_k(x) > 0$ for all x on (x_1, x_2)

That is, no solid concentration vanishes on (x_1, x_2), unless that solid is entirely absent from the interval. Hence the solid identities are invariant on (x_1, x_2), even though the solid concentrations need not be. Since the solubility product constraint Eq. 4 is independent of solid concentration, the same set of solubility product constraints applies throughout an IISI.

The covering postulate means that at any given time we may divide the distance axis into N open intervals (x_n, x_{n+1}), $n = 1, \ldots, N$, with $x_1 = 0$ and $x_{N+1} = L$, each of which satisfies the invariance condition above. A covering that contains four IISI appears in Figure 1. The intervals $(0, x_2)$ and (x_3, x_4) contain the solids S_1, S_3, S_4. The interval (x_2, x_3) contains the solids S_1, S_2, S_3, and S_4. The interval (x_4, L) contains the solids S_1 and S_4. The horizontal axis in Figure 1 is dimensional.

An IISI that exists for any length of time traces out a finite area in time-distance space. For example, suppose that at time t_0 K solids are present at concentrations $\{\underline{C}_k(x), k = 1, \ldots, K\}$ in the space interval (x_1^0, x_2^0) with $x_1^0 < x_2^0$. Suppose further that the end points of the interval move through the medium along nonintersecting curves $x_1 = x_1(t)$ and $x_2 = x_2(t)$ during the time interval (t_0, t_1). This movement defines a region in time-distance space in which the solid identities are invariant (a RISI). Thus the flowing phase concentrations satisfy the solubility products of the K solids everywhere in this RISI.

Characteristics and Riemann invariants in the flowing phase

Within a RISI we can define characteristics and Riemann invariants very simply because of the peculiar nature of the solubility product constraint. Rewrite Eq. 8 on an arbitrary RISI (denoted R) as

$$\partial C_i/\partial t + \partial C_i/\partial x = -\partial(g_{ik}\underline{C}_k)/\partial t \quad i = 1, \ldots, I \quad (12)$$

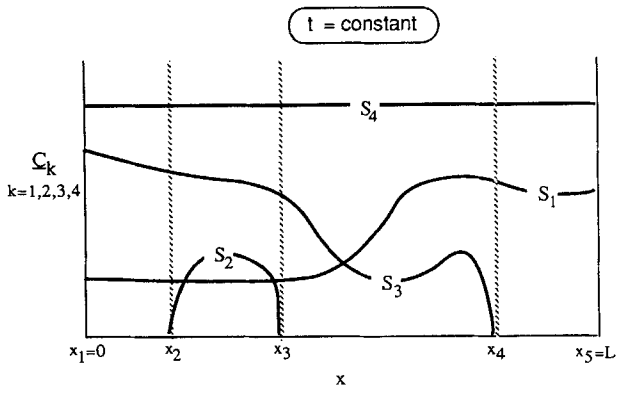

Figure 1. Intervals of invariant solid identities cover the distance axis at any time in a precipitation/dissolution problem.

S_k is solid species k with concentration $\underline{C}_k$

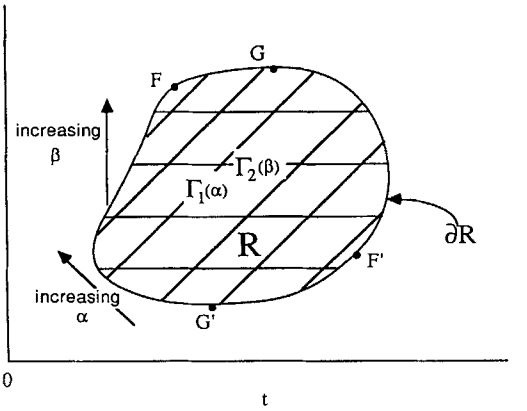

Figure 2. Flowing phase Γ_1 and solid phase Γ_2 characteristics in an arbitrary region R of invariant solid identities.

The solid phase concentrations can be eliminated algebraically from Eq. 12 as we now demonstrate. In matrix form Eq. 12 becomes

$$L_1(C) = [g_{ik}]L_2(\underline{C}) \tag{13}$$

Because the matrix $[g_{ik}]$ has rank K_R, the number of solids present in R, we may reduce Eq. 13 to a set of K_R inhomogeneous equations

$$L_1(UC) = U[g_{ik}]L_2(\underline{C}) \tag{14}$$

and a set of $I - K_R$ homogeneous equations

$$L_1(VC) = (0) \tag{15}$$

where U is a $K_R \times I$ matrix with elements u_{ti}, $t = 1, \ldots, K_R$, $i = 1, \ldots, I$; V is an $(I - K_R) \times I$ matrix with elements ν_{si}, $s = 1, \ldots, (I - K_R)$, $i = 1, \ldots, I$; and (0) represents the $(I - K_R)$-element zero vector. Matrices U and V represent algebraic manipulations of the rows of $[g_{ik}]$. Equation 15 contains no solid concentrations, as desired.

The product VC in Eq. 15 defines $(I - K_R)$ linear combinations of the I total flowing phase concentrations C_i, which we express as $\nu_{si}C_i$. Equation 15 implies that L_1 conserves each of these combinations in region R. The constants ν_{si} are linear combinations of the stoichiometric coefficients g_{ik} and thus depend on the solid identities in R, but not on the solid concentrations there.

Defining quantities $X_s = \nu_{si}C_i$, we solve Eq. 15 immediately by

$$X_s = \chi_s(x - t) \quad s = 1, \ldots, I - K_R \tag{16}$$

where χ_s is an arbitrary function satisfying appropriate boundary data. From the form of Eq. 16, X_s is constant along any curve in R satisfying $x - t =$ constant. This relation defines a family Γ_1 of characteristics in R (Lax, 1957; Whitham, 1974; Taniuiti and Nishihara, 1983), where $\Gamma_1(\alpha)$ denotes the curve given by $x - t = \alpha$. Figure 2 depicts this family in region R; on dimensionless time-distance axes the Γ_1 have unit slope. The $I - K_R$ variables X_s are by definition components of a Riemann invariant, $J_1 = (X_1, X_2, \ldots, X_{I-K_R})$, in region R. The flowing phase invariant J_1 is particular to region R, for elimination of a different set of solids in a different RISI will, in general, result in a different set of X_s. Values of J_1 are transported unchanged along the characteristics Γ_1.

To determine J_1 on R, consider a segment $FG'F'$ of ∂R, the boundary of R, to which each point in R can be connected by a characteristic $\Gamma_1(\alpha)$, Figure 2. Since J_1 does not change along a characteristic, fixing the value of J_1 on $FG'F'$ determines J_1 on the entire region R. Thus if J_1 is constant on the boundary $FG'F'$, it is constant on all of R.

Determining the flowing phase invariant J_1 on R determines the total flowing phase concentrations C_i on R. K_R solubility products, $\{K_k^{sp}; k = 1, \ldots, K_R\}$, constrain the flowing phase concentration on R; there is one solubility product for each solid eliminated from Eq. 12. Fixing values for the X_s and the K_k^{sp} provides a total of $(I - K_R) + K_R = I$ constraints that determine the total flowing phase concentrations:

$$C_i = C_i(X_s; K_k^{sp}) \quad i = 1, \ldots, I \tag{17}$$

The semicolon in Eq. 17 separates the (x, t)-dependent variables X_s from the parameters K_k^{sp}.

Characteristics and Riemann invariants in the solid phase

The flowing phase invariant J_1 leads to an invariant that involves only the solid concentrations. Substitution of Eq. 17 into conservation Eq. 12 yields

$$(\partial C_i/\partial X_s)[\partial X_s/\partial t + \partial X_s/\partial x] = -\partial(g_{ik}\underline{C}_k)/\partial t \quad i = 1, \ldots, I \tag{18}$$

According to Eq. 16, the left side of Eq. 18 is identically zero, and we have

$$g_{ik}(\partial \underline{C}_k/\partial t) = 0 \quad i = 1, \ldots, I \tag{19}$$

We immediately solve Eq. 19 by

$$\underline{C}_k = \theta_k(x) \quad k = 1, \ldots, K_R \tag{20}$$

where θ_k is an arbitrary function satisfying appropriate boundary data. From the form of Eq. 20 $\underline{C}_k$ is constant along any curve in R satisfying x = constant. This relation defines a family Γ_2 of characteristics in which $\Gamma_2(\beta)$ denotes the curve in R given by $x = \beta$. Figure 2 depicts this family; on dimensionless time-distance axes these characteristics have zero slope. The K_R variables $\underline{C}_k$ comprise another Riemann invariant, $J_2 = (\underline{C}_1, \underline{C}_2, \ldots, \underline{C}_{K_R})$, in region R. Like J_1, J_2 is particular to region R. Values of J_2 are transported unchanged along the characteristics Γ_2. To determine J_2 on R, it suffices to evaluate it on some segment GFG' of ∂R to which all points in R are connected by $\Gamma_2(\beta)$.

Form of the solution of the precipitation/dissolution problem

The covering postulate suggests that the solution of Eq. 8 will consist of RISI connecting the initial conditions (the distance axis) and injected conditions (the time axis), Figure 3. For Riemann conditions, the boundaries of these RISI must emanate from the origin of the time-distance axes. These boundaries mark changes in solid identities that are accompanied by changes in concentrations. Thus these boundaries are waves: concentration changes moving through the permeable medium. All waves have slope everywhere less than or equal to unity, lest they violate the second law of thermodynamics (Bryant, 1986).

In general, the flowing phase and solid invariants in each interior sector R^n differ from the invariants in adjacent sectors because different solids will be present in each sector. We will relate the values of the invariants in adjacent sectors via mass balances at the boundary between the sectors.

Because the Γ_1 have unit slope, they must originate from the upstream boundary of any interior sector R^n. Since the Γ_2 have zero slope, they must originate from the downstream boundary of any interior sector. Consequently the calculation of the flowing phase invariants will proceed in the downstream direction, beginning with the injected conditions sector R^J. Conversely the calculation of the solid invariants will proceed in the upstream direction, beginning with the initial conditions sector R^0. This bi-directional calculation is unique to the precipitation/dissolution problem and the solubility product constraint; in chromatography, for example, both phase compositions are calculated together in the same direction.

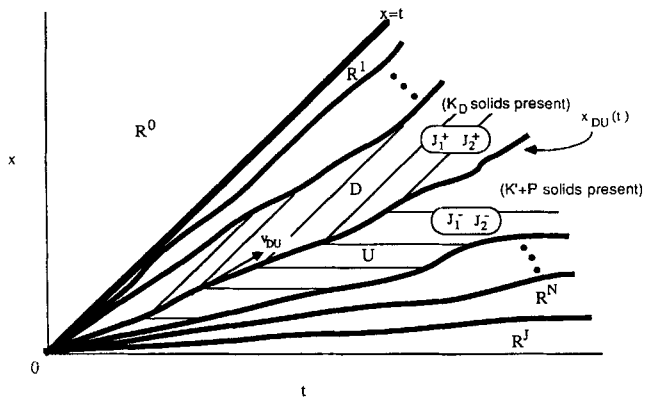

Figure 3. Solution to general precipitation/dissolution problem should consist of regions of invariant solid identities, R^0, R^1, . . . , R^J separated by waves (heavy lines).

From $D - U$ boundary flowing phase characteristics emanate in sector D, solid phase characteristics in sector U
J_1^+, J_1^-, flowing phase invariants; J_2^+, J_2^-, solid phase invariants

The general precipitation/dissolution wave

To calculate the invariants in the sectors in Figure 3, we must examine the relations between invariants at boundaries between sectors; i.e., at precipitation/dissolution waves. Let regions D and U be RISI downstream and upstream, respectively, of an arbitrary wave in the proposed solution, shown in Figure 3. Let some function $x_{DU}(t)$ define the $D - U$ boundary in time-distance space, so that $v_{DU}(t) = dx_{DU}/dt$ is the specific velocity of the $D - U$ wave. Let K_D be the number of solids in region D. Let P be the number of solids in region U that are not in D. These P solids are just those that precipitate across the wave. Thus there are a total of $K_D + P$ distinct solids in sectors D and U. Let K' be the number of solids in U that are also in D. At least one solid must completely dissolve across any precipitation/dissolution wave (Bryant, 1986), so $K_D > K'$. Then region U contains a total of $K' + P$ solids, and $K_D - K'$ solids completely dissolve across this zero-dissipation precipitation/dissolution wave.

Let I be the number of elements that compose the $K_D + P$ distinct solids. As discussed in connection with Eq. 5, the number of independent species always exceeds the number of solids at any position in the medium. Thus, we have that $I > K_D$ and $I > K' + P$, whence $I > P$. However, it is possible that $I \leq K_D + P$, even though $I > K_D$ and $I > P$.

Relating the invariants across the wave

In sector D the flowing phase invariant J_1^+ has $I - K_D$ components, Eq. 16; the solid phase invariant J_2^+ has K_D components, Eq. 20. In sector U the flowing phase invariant J_1^- has $I - K' - P$ components, and the solid phase invariant J_2^- has $K' + P$ components. Because the flowing phase characteristics in D propagate from the $D - U$ boundary, we anticipate calculating J_1^+ in terms of J_1^-. That is, we will relate the concentrations $\{C_i^+, i = 1, \ldots, I\}$ in D to the concentrations $\{C_i^-, i = 1, \ldots, I\}$ in U.

Because the solid characteristics in U propagate from the $D - U$ boundary, we calculate J_2^- in terms of J_2^+, relating the concentrations $\{\underline{C}_k^-, k = 1, \ldots, K' + P\}$ in U to the concentrations $\{\underline{C}_k^+, k = 1, \ldots, K_D\}$ in D. In the absence of dissipation, all concentrations undergo step changes at the $D - U$ boundary; i.e., a precipitation/dissolution wave is a shock. Hence we apply the integral form of the mass balance, Eq. 10, at the boundary to calculate J_1^+ and J_2^-. We have

$$v_{DU} = (1 + \Delta g_{ik} \underline{C}_k / \Delta C_i)^{-1} \tag{21}$$

The concentration jumps ΔX in Eq. 21 are evaluated across the $D - U$ boundary.

Coherence

The wave represented by the $D - U$ boundary is coherent; that is, the velocity of each independent species concentration is the same in the wave (Helfferich and Klein, 1970). The mass balance represented by Eq. 21 applies to each of the I independent species. The boundary between D and U is simply the mathematical locus of points given by the function $x_{DU}(t)$. Consequently the velocity $v_{DU} = dx_{DU}/dt$ is quite independent of which independent species A_i' appears in Eq. 21. Therefore the same

value for v_{DU} must result from each of the I mass balances:

$$v_{DU} = (1 + \Delta g_{1k}\underline{C}_k/\Delta C_1)^{-1} = (1 + \Delta g_{2k}\underline{C}_k/\Delta C_2)^{-1} = \cdots = (1 + \Delta g_{Ik}\underline{C}_k/\Delta C_I)^{-1} \quad (22)$$

Equation 22 is just the definition of coherence.

The fundamental assumption in the derivation of Eq. 22 is the covering postulate. Thus the existence of IISI implies coherence of precipitation/dissolution waves. A noncoherent wave could occur only within a noninvariant open interval in which a different set of solids existed at every point.

Determining J_1^+ *when* $I > K_D + P$

First consider the case when the number of independent species in the wave, I, exceeds the number of distinct solids upstream and downstream of the wave, $(K_D + P)$. We regard Eq. 22 first as a system of equations for the unknown flowing phase concentrations in D, or equivalently for J_1^+. Since the solid concentrations can be eliminated from the differential mass balances, Eq. 12, a similar elimination of solids from Eq. 22 should be possible. Solving for $\Delta\underline{C}_i$ in Eq. 22 yields I discrete mass balances:

$$\Delta C_i = [v_{DU}/(1 - v_{DU})]\Delta g_{ik}\underline{C}_k \quad i = 1, \ldots, I$$

which becomes in matrix form:

$$\Delta C = [v_{DU}/(1 - v_{DU})][g_{ik}]\Delta\underline{C} \quad (23)$$

where C, $[g_{ik}]$, and $\underline{C}$ are as in Eq. 13, except that here $[g_{ik}]$ has dimension $I \times (K_D + P)$ and $\underline{C}$ is the $(K_D + P)$ vector of the distinct solid concentrations in D and U. Equation 23 is analogous to Eq. 13 with the discrete operators Δ and $[v_{DU}/(1 - v_{DU})]\Delta$ corresponding to the differential operators L_1 and L_2, respectively. Since $I > K_D + P$, the scheme that reduces Eq. 13 to Eqs. 14 and 15 applies to Eq. 23. A set of $K_D + P$ inhomogeneous equations and a set of $I - (K_D + P)$ homogeneous equations result:

$$U'\Delta C = [v_{DU}/(1 - v_{DU})]U'[g_{ik}]\Delta\underline{C}$$

and

$$V'\Delta C = (0) \quad (24)$$

where U' has dimension $K_D + P$ by I and V' has dimension $I - (K_D + P)$ by I.

The homogeneous set of Eqs. 24 is equivalent to

$$V'C_i^+ = V'C_i^- \quad i = 1, \ldots, I - (K_D + P) \quad (25)$$

Neither the solid concentrations nor the velocity v_{DU} appear in Eq. 25, the "reduced coherence conditions." The C_i^+ are functions of the $I - K_D$ components of J_1^+, and the C_i^- are functions of the $I - K' - P$ components of J_1^-. If $P = 0$, the wave is a dissolution-only wave, and Eq. 25 determines the J_1^+ in terms of the J_1^-. If $P > 0$ the $I - (K_D + P)$ equations, Eq. 25, are sufficient; an additional set of P equations is required to determine J_1^+. The missing equations are a fundamental feature of the precipitation/dissolution wave.

Jump Conditions and the Wave in the Presence of Dissipation. Similar indeterminacies arise in other systems of hyperbolic conservation equations when shocks in the conserved variables occur (Rhee et al., 1970; Whitham, 1974; Taniuti and Nishihara, 1983). The additional equations that must be supplied to determine the solution are often called evolution or jump conditions.

To obtain jump conditions for the precipitation/dissolution wave, we will determine the concentration profile of the wave in the presence of dissipation, what Whitham (1974) calls its "shock structure." Certain properties of the wave that cannot be derived in the absence of dissipation may become apparent in the shock structure. These properties provide jump conditions for the wave if they hold in the limit of zero dissipation.

It is convenient to define a reference frame moving with the wave by $z = x - v_{DU}t$. In this frame, dissipative conservation Eq. 6 becomes

$$\partial C_i^T/\partial t - (v_{DU} + td v_{DU}/dt)\partial C_i^T/\partial z + \partial C_i/\partial z - (N_{Pe})^{-1}\partial^2 C_i/\partial z^2 = 0 \quad i = 1, \ldots, I \quad (26)$$

At sufficiently large time ($t = t_{large}$), the profile of a shock attains a constant pattern (Lake and Helfferich, 1978). Thus the time derivatives vanish in Eq. 26, yielding:

$$L_3\{C_i\} = v_{DU}d/dz(g_{ik}\underline{C}_k)\ t > t_{large} \quad i = 1, \ldots, I$$

where we separate C_i^T into its flowing phase and solid cont tions, as in Eq. 12.

Profile in an IISI Moving with the Wave. Before exam the structure of the $D - U$ wave, we first derive the local b ior of Eq. 27 on an arbitrary IISI (z_1, z_2). We take z_1 and z_2 constant, so the IISI moves through the medium at the velocity as the wave. Elimination of the solid concentra from Eq. 27 yields

$$L_3\{\nu_{si}C_i\} = 0, z_1 < z < z_2, t > t_{large} \quad s = 1, \ldots, I - K_z \quad (28)$$

where K_z is the number of solids in the interval (z_1, z_2). Equation 28 implies that L_3 conserves the quantities $\nu_{si}C_i$ in (z_1, z_2), which are formally identical to the invariant components found in region R, Eq. 16.

Integrating Eq. 28 twice yields

$$\nu_{si}C_i = \alpha_s + \beta_s \exp(bz), z_1 < z < z_2, t > t_{large} \quad s = 1, \ldots, I - K_z \quad (29)$$

where $b = (1 - v_{DU})N_{Pe}$. Since the specific wave velocity v_{DU} must be less than unity, $b > 0$. The K_z solubility products and the $I - K_z$ equations of Eq. 29 determine the flowing phase concentrations C_i on (z_1, z_2) up to the constants α_s and β_s, $s = 1, \ldots, I - K_z$. In contrast to the zero-dissipation solution on a RISI given by Eq. 16, Eq. 29 displays an exponential dependence of flowing phase concentration on distance in this IISI.

We have seen that I mass balances involving K solids contain only K independent equations in the K solid concentrations, Eq. 14. Thus we may solve Eq. 27 for the K_z unknowns $d\underline{C}_k/dz$:

$$d\underline{C}_k/dz = L_3\{\eta_{ki}C_i\}, z_1 < z < z_2, t > t_{large} \quad k = 1, \ldots, K_z \quad (30)$$

where η_{ki} are constants arising from matrix row operations. In general $L_3\{\eta_{ki}C_i\}$ is nonzero due to Eq. 29, so Eq. 30 is not a

homogeneous system, also in contrast to the zero-dissipation case (cf. Eq. 19). Integrating Eq. 30 yields an expression for the solid concentrations that retains the exponential dependence upon distance from the wave:

$$\underline{C}_k = \gamma_k + (1 - v_{DU})(\eta_{ki}C_i) - (N_{Pe}^{-1})d(\eta_{ki}C_i)/dz \cdot z_1 < z < z_2, t > t_{large} \quad k = 1, \ldots, K_z \quad (31)$$

where γ_k are constants of integration.

Profile of a Semiinfinite IISI Moving with the Wave. The form of Eq. 29 immediately leads to a useful restriction on the concentration profiles on a semiinfinite IISI $(z_1, +\infty)$. Since $b > 0$, the constants β_s must be identically zero, else the concentrations would diverge as $z_2 \rightarrow +\infty$. Thus $\nu_{si}C_i$ is independent of z on $(z_1, +\infty)$ for all s:

$$\nu_{si}C_i = \alpha_s, z_1 < z < +\infty \quad t > t_{large} \quad s = 1, \ldots, I - K_z \quad (32)$$

Now the K_z solubility products and the $J - I$ homogeneous equilibria that constrain the flowing phase concentrations are independent of z on $(z_1, +\infty)$. Therefore the flowing phase composition must be constant on (z_1, ∞). Substitution of this constant composition into Eq. 31 shows that all solid concentrations are also constant:

$$\underline{C}_k = \gamma_k + (1 - v_{DU})(\eta_{ki}C_i), z_1 < z < +\infty, t > t_{large} \quad k = 1, \ldots, K_z \quad (33)$$

Hence a semiinfinite interval $(z_1, +\infty)$ of invariant solid identities must be a constant state.

Complete Profile of the Wave. The sectors D and U extend indefinitely into the $x - t$ quadrant, so at some time $t_{large} \rightarrow +\infty$ the precipitation/dissolution wave will appear as an isolated disturbance between two very long constant-state regions. Therefore the shock structure of the wave approaches boundary conditions of the form:

$$C_i \rightarrow C_i^+; \underline{C}_k \rightarrow \underline{C}_k^+ \text{ at } t = t_{large} \text{ as } z \rightarrow +\infty \quad i = 1, \ldots, I; k = 1, \ldots, K_D$$

$$C_i \rightarrow C_i^-; \underline{C}_k \rightarrow \underline{C}_k^- \text{ at } t = t_{large} \text{ as } z \rightarrow +\infty \quad i = 1, \ldots, I; k = 1, \ldots, K' + P \quad (34)$$

Since Eq. 27 is second order, a third boundary condition is needed in addition to Eq. 34. The flowing phase concentration profiles must be continuous in the presence of dissipation, otherwise infinite dissipative fluxes arise, Eq. 7. We use this continuity as the third boundary condition.

Although the flowing phase concentrations are continuous in the presence of dissipation, the appearance of a solid at any position z introduces a discontinuity at z in the solid concentrations and in the derivative of the flowing phase concentrations (Bryant, 1986). (We henceforth use the term "discontinuity" to mean such a discontinuity in a concentration profile.) Thus the profile of a precipitation/dissolution wave necessarily exhibits a discontinuity, and differential conservative equations, Eq. 27, cannot apply uniformly across the wave from $-\infty < z < \infty$. However, according to the covering postulate IISI can always be found around any discontinuity. We will therefore piece together the precipitation/dissolution wave profile from Eqs. 29 and 31 on individual IISI comprising the wave.

The single-discontinuity wave

Suppose that exactly one solid completely dissolves across the wave, so a single discontinuity occurs in the shock structure. Thus no IISI intervene between the upstream and downstream IISI corresponding to sectors U and D, Figure 4. Identify the origin of the moving coordinate frame $(z = 0)$ with the single discontinuity in the wave, as in Figure 4. The semiinfinite interval $(0, +\infty)$ must be a single IISI. If it were not, a solid would appear or disappear at some point $z^* > 0$, thereby inducing a second discontinuity. Thus the constant-state solution of Eqs. 32 and 33 applies in $(0, +\infty)$. Using boundary conditions Eq. 34 to evaluate the constants in these equations, we have

$$C_i(z) = C_i^+; \underline{C}_k(z) = \underline{C}_k^+, 0 < z < +\infty, t = t_{large}, \quad i = 1, \ldots, I; k = 1, \ldots, K_D \quad (35)$$

Upstream of the discontinuity, i.e., the interval $(-\infty, 0)$, the concentration profiles take the form of Eqs. 29 and 31:

$$\nu_{si}C_i = \alpha_s + \beta_s \exp(bz), -\infty < z < 0 \; t = t_{large}, \quad s = 1, \ldots, I - K' - P$$

$$\underline{C}_k = \gamma_k + (1 - v_{DU})(\eta_{ki}C_i) - (N_{Pe}^{-1})d(\eta_{ki}C_i)/dz \quad -\infty < z < 0, t = t_{large}, \quad k = 1, \ldots, K' + P \quad (36)$$

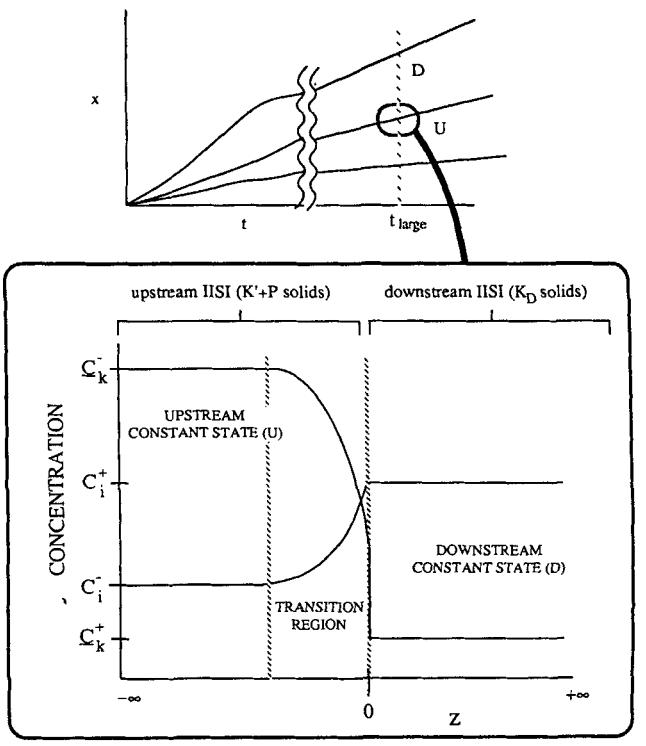

Figure 4. Shock structure of a precipitation/dissolution wave for $I > K_D + P$ attains a constant pattern asymptotically.

Concentration profiles exhibit a single discontinuity at $z = 0$ that separates two intervals of invariant solid identities

As shown in Figure 4, the concentration profiles at large time exhibit

- A region of essentially constant concentration far upstream of the wave where the exponential term in Eq. 36 is negligible
- A transition region in which the concentrations vary with the exponential of distance
- A constant state region downstream of the wave
- A discontinuity between the transition region and the constant downstream state.

It remains to evaluate the constants of integration in Eq. 36, α_s, β_s, and γ_k. Since $b > 0$, all exponential terms in Eq. 36 vanish as $z \Longrightarrow -\infty$. This limit together with the boundary conditions Eq. 34 determines the constants α_s and γ_k:

$$\alpha_s = \nu_{si} C_i^- \qquad s = 1, \ldots, I - K' - P$$
$$\gamma_k = \underline{C}_k^- - (1 - v_{DU})(\eta_{ki} C_i^-) \qquad k = 1, \ldots, K' + P \tag{37}$$

The flowing phase concentrations must be continuous everywhere and in particular at $z = 0$. This requirement provides I matching conditions:

$$C_i(0^-) = C_i(0^+) = C_i^+ \qquad i = 1, \ldots, I \tag{38}$$

where the concentrations on the left side of Eq. 38 are determined by Eq. 36 and the $K' + P$ solubility products in U (cf. Eq. 17), and we have substituted Eq. 35 on the right side. Now only $I - K'$ of the matching conditions of Eq. 38 are independent. This is because K' solids are present in both the upstream and downstream IISI, so the flowing phase concentrations on both sides of $z = 0$ satisfy K' solubility products.

Since Eq. 37 determines the $I - K' - P$ constants α_s, Eq. 38 involves only $I - K' - P$ undetermined constants of integration, the β_s. Forming the linear combinations $\nu_{si} C_i$, $s = 1, \ldots, I - K' - P$, from Eq. 38 yields

$$\nu_{si} C_i(0^-) = \nu_{si} C_i^+ \qquad s = 1, \ldots, I - K' - P \tag{39}$$

Substituting Eq. 36 for the left side of Eq. 39 yields

$$\alpha_s + \beta_s = \nu_{si} C_i^+ \qquad s = 1, \ldots, I - K' - P$$

which becomes

$$\beta_s = \nu_{si}(C_i^+ - C_i^-) \qquad s = 1, \ldots, I - K' - P \tag{40}$$

when Eq. 37 is applied.

Equation 40 in effect determines $I - K' - P$ of the matching conditions in terms of the others. Thus $(I - K') - (I - K' - P) = P$ of the original matching conditions, Eq. 38, remain independent and unused.

The Downstream Equilibrium Condition. These P equations impose additional relations, not on the constants of integration, but on the downstream flowing phase concentrations C_i^+. The flowing phase concentrations just upstream of the discontinuity, $C_i(0^-)$, satisfy the $K' + P$ solubility products of the upstream solids. Matching the flowing phase concentrations at $z = 0$ means that the flowing phase concentrations just downstream of the discontinuity, C_i^+, will also satisfy these $K' + P$ solubility products. Since the interval downstream of the discontinuity is a constant state, the flowing phase concentrations throughout the downstream interval satisfy the $K' + P$ solubility products of the upstream solids.

Since K' solids are present downstream as well as upstream of the wave, the C_i^+ already satisfy the K' solubility products because of local equilibrium. However, by definition the P solids that precipitate across the wave are not present downstream, so local equilibrium would not require the downstream concentrations C_i^+ to satisfy the solubility products of these solids. The matching conditions therefore constrain the C_i^+ with P additional solubility products.

This result extends the weaker requirement of local equilibrium. Since the K_D, K', and P solids are arbitrary subject to the constraint that $I > K_D + P$, we may state that in the presence of dissipation,

> Throughout the constant-state region downstream of a single-discontinuity precipitation/dissolution wave, the flowing phase concentrations satisfy the solubility products of the solids upstream of the wave, regardless of whether any upstream solids are actually present downstream.

This result is the downstream equilibrium condition (DEC), suggested but not rigorously proved by Walsh et al. (1984). A graphical depiction of the DEC for a simple precipitation/dissolution wave appears in Figure 5.

Proof of the DEC required nonzero dissipation, so we cannot derive the DEC from zero-dissipation conservation Eqs. 8. However, we expect that it is preserved as a jump condition in the limit of zero dissipation. That the DEC provides precisely the number of jump conditions needed in the zero-dissipation problem strongly supports this expectation. Furthermore the shock structure, Eqs. 35 and 36, approaches the zero-dissipation profile (a step change between C_i^+ and C_i^-) as the dissipation coefficient goes to zero. To see this, recall that $b = (1 - v_{DU})N_{Pe} = (1 - v_{DU})uL/D_0\phi$. Thus

$$\lim_{D_0 \to 0} [\alpha_s + \beta_s \exp(bz)] = \alpha_s \quad \text{for any } z \in (-\infty, 0)$$

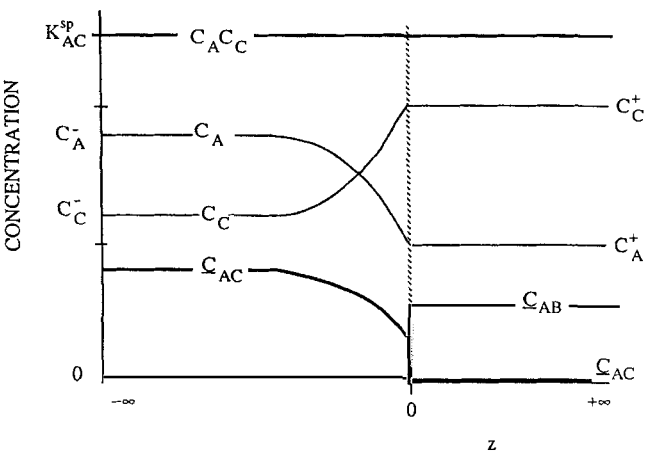

Figure 5. Downstream equilibrium condition for an *AC*-precipitation/*AB*-dissolution wave.

Across transition region, concentrations of A and C change from constant upstream values to constant downstream values. However, the product of these concentrations does not change, so the solubility product for solid AC is satisfied even though AC is not present downstream.

Numerical confirmation of the single-discontinuity shock structure and the DEC appears in the Appendix.

The DEC coupled with the reduced coherence conditions, Eq. 25, determines J_1^+ in terms of J_1^- in the absence of dissipation.

Determining J_2^- *when* $I > K_D + P$

To relate the solid invariants across the wave, we solve the original coherence conditions, Eq. 22, for the $\Delta\underline{C}_k$, thereby expressing J_2^- in terms of J_2^+. Eliminating the velocity v_{DU} from Eq. 22 yields $I - 1$ equations:

$$\Delta g_{1k}\underline{C}_k/\Delta C_1 = \Delta g_{2k}\underline{C}_k/\Delta C_2 = \cdots = \Delta g_{Ik}\underline{C}_k/\Delta C_I \qquad (41)$$

Since we have determined J_1^+ in terms of J_1^-, the ΔC_i are known, and we rewrite Eq. 41 as a system of equations in terms of the $\Delta\underline{C}_k$. In matrix form this system is

$$G\Delta\underline{C} = (0) \qquad (42)$$

where G is a matrix of dimension $(I - 1) \times (K_D + P)$ with elements $G_{ik} = [g_{ik}/\Delta C_i] - [g_{i+1,k}/\Delta C_{i+1}]$, $i = 1, \ldots, I - 1$; $k = 1, \ldots, K_D + P$. Without loss of generality we may assume $\Delta\underline{C}_i \neq 0$ for $i = 1, \ldots, I$, so G is well defined (Bryant, 1986). Because the trivial solution $\Delta\underline{C} = (0)$ is a degenerate case for precipitation/dissolution waves, we seek a nontrivial solution to Eq. 42.

Matrix G has rank $K_D + P - 1$ (Bryant, 1986), so Eq. 42 provides only $K_D + P - 1$ independent equations for the $K_D + P$ unknown $\Delta\underline{C}_k$:

$$G'\Delta\underline{C} = (0) \qquad (43)$$

where G' is a nonsingular submatrix of dimension $K_D + P - 1$ by $K_D + P$. Since Eq. 43 is a homogeneous system in the unknown solid concentration changes, we must find one inhomogeneous equation in the $\Delta\underline{C}_k$ to obtain a nontrivial solution. Since exactly one solid completely dissolves across a single-discontinuity wave, the concentration of exactly one of the K_D downstream solids, say solid S_{K^*}, is zero in the upstream region U; i.e., $\underline{C}_{K^*}^- = 0$. Then a new equation restricts the $\Delta\underline{C}_k$, namely

$$\Delta\underline{C}_{K^*} = \underline{C}_{K^*}^+ - \underline{C}_{K^*}^- = \underline{C}_{K^*}^+ \qquad (44)$$

Since $\underline{C}_{K^*}^+$ is nonzero, Eqs. 43 and 44 yield an inhomogeneous system of $K_D + P - 1$ equations that determines the remaining $K_D + P - 1$ solid concentration changes $\Delta\underline{C}_k$. The upstream solid concentrations are then calculated from $\underline{C}_k^- = \underline{C}_k^+ - \Delta\underline{C}_k$.

At this point we have determined J_1^+ and J_2^- in terms of J_1^- and J_2^+ for the single-discontinuity precipitation/dissolution wave in the absence of dissipation when $I > K_D + P$.

Multiple-discontinuity waves

Some precipitation/dissolution waves must exhibit more than one discontinuity in their shock structure because the DEC leads to contradictions in the zero-dissipation limit. In one class of multiple-discontinuity waves the DEC would overconstrain the downstream flowing phase concentrations. In the other class of multiple-discontinuity waves, the DEC would force the wave to be noncoherent. We treat the two classes individually.

Relating the invariants when $I \leq K_D + P$

The first class is characterized by the presence of more distinct solids than independent species in the wave; i.e., $I \leq K_D + P$ or equivalently, $K_D + P > I - 1$. This case immediately introduces conflicts in the solutions for J_1^+ and J_2^- described above. First, in the zero-dissipation solution, the reduction of the coherence conditions to Eq. 25 is not possible when $K_D + P > I - 1$, for matrix V' cannot exist.

Second, in the single-discontinuity wave structure the DEC and local equilibrium impose a total of $K_D + P$ solubility products on the C_i^+ in sector D. When $K_D + P > I - 1$, the C_i^+ are overconstrained by the solubility products and the electroneutrality condition. A convenient measure of overconstraint, denoted ρ, is the difference between the number of constraints on the downstream flowing phase concentrations (assuming a single-discontinuity wave) and the number of independent flowing phase concentrations: $\rho = (K_D + P + 1) - I$. If $\rho \leq 0$, then $I > K_D + P$, and the DEC does not overconstrain the C_i^+. If $\rho > 0$, the DEC provides ρ more equations across the wave than the downstream concentrations can satisfy, and we must modify our solution procedure for J_1^+ and J_2^-.

Determining J_1^+ *for* $\rho > 0$. We again seek $I - K_D$ equations free of solid concentrations to determine the components of J_1^+ in terms of J_1^-. We will need the mass flux balances with respect to v_{DU} at an arbitrary point in the vicinity of the wave. These have the form:

$$(1 - v_{DU})C_i - (N_{Pe})^{-1}dC_i/dz - v_{DU}(g_{ik}\underline{C}_k) = \phi_i \qquad i = 1, \ldots, I \qquad (45)$$

where ϕ is a constant.

The coherence conditions, Eq. 22, apply regardless of the value of ρ, and they imply the flowing phase charge balance across the wave (Bryant, 1986):

$$w_j\Delta C_j = 0 \qquad (46)$$

Since $I < K_D + P + 1$, reduction of the coherence equations is impossible, and the remaining $I - K_D - 1$ equations needed to determine J_1^+ must be jump conditions. Thus we must consider the shock structure of the wave for $\rho > 0$.

The coherence conditions in the form of Eq. 42 provide insight into this shock structure. To determine the $(K_D + P)$ $\Delta\underline{C}_k$, we need $K_D + P$ equations. Equation 42 provides $I - 2$ linearly independent homogeneous equations in the solid concentration changes $\Delta\underline{C}_k$ if $\rho > 0$ (Bryant, 1986). Complete dissolution of $\rho + 1$ of the K_D downstream solids provides $\rho + 1$ inhomogeneous equations like Eq. 44. This yields a total of $I - 2 + \rho + 1 = K_D + P$ equations, which determine the $\Delta\underline{C}_k$. Since $\rho > 0$, then $\rho + 1 > 1$, which means that at least two solids in D must completely dissolve across the wave. This contrasts with the case for single-discontinuity waves, wherein dissolution of two solids in D would impose incompatible constraints on the matrix G' in Eq. 43.

Only one solid can completely dissolve at any given point without overconstraining the mass flux balances, Eq. 45. Since $\rho + 1$ solids completely dissolve across the wave, there must be $\rho + 1$ points $z_n (n = 0, \ldots, \rho; z_0 = 0)$ in the wave profile that separate the upstream and downstream constant states with ρ distinct IISI, Figure 6. At $t = t_{large}$ each z_n must be stationary in the moving reference frame because the wave attains a constant

pattern. Thus, when $\rho > 0$ the shock structure of the wave exhibits $\rho + 1$ subregions within the transition region compared to the single transition region in the single-discontinuity wave. The composition in each interval (z_{n+1}, z_n) and on $(-\infty, z_\rho)$ is given by Eq. 36 and the solubility products of the solids in each interval:

$$
\begin{aligned}
(\nu_{si} C_i)^{(n)} &= \alpha_s^{(n)} + \beta_s^{(n)} \exp(bz), \quad s = 1, \ldots, I - K' - P \\
\underline{C}_k^{(n)} &= \gamma_k^{(n)} + (1 - v_{DU})(\eta_{ki} C_i)^{(n)} \\
&\quad - (N_{Pe}^{-1})\, d(\eta_{ki} C_i)^{(n)}/dz \\
&\quad \cdot z_{n+1} < z < z_n,\ t = t_{large} \quad k = 1, \ldots, K' + P
\end{aligned} \tag{47}
$$

The semiinfinite interval $(0, +\infty)$ corresponding to region D is a constant state, Eq. 35.

The first subregion upstream of D, the interval $(z_1, 0)$ in Figure 6, provides jump conditions for determining J_1^+ in the absence of dissipation. Continuity of the flowing phase concentrations at $z = 0$ implies that the solubility products of the solids in $(z_1, 0)$ will be satisfied in the constant state region D.

If $K_D = I - 1$, then the number of jump conditions needed ($= I - 1 - K_D$) is zero. In this case the flowing phase concentrations C_i^+ in D are completely determined by Eq. 46 and local equilibrium. Thus no solids could precipitate at $z = 0$.

However, if $K_D < I - 1$, then $P_1 = I - 1 - K_D$ solids can precipitate at $z = 0$. Since we are considering the case $I \le K_D + P$, we have $P_1 < P$, and the C_i^+ satisfy the solubility products of a subset of the P precipitates in region U. This is a weaker form of the DEC, a partial downstream equilibrium condition (PDEC), Figure 6. The PDEC provides $P_1 = I - 1 - K_D$ jump conditions that, combined with Eq. 46, determine J_1^+ in the absence of dissipation.

Determining J_2^- *for* $\rho > 0$. The coherence conditions, Eq. 42, and complete dissolution of $\rho + 1$ solids provide $(I - 2) + (\rho + 1) = K_D + P$ equations that determine the $\Delta \underline{C}_k$ in terms of the ΔC_i. At this point we have J_2^- and J_1^+ for the precipitation/dissolution wave when $I \le K_D + P$.

The Intervening IISI in the Shock Structure for $\rho > 0$. For completeness we describe the profiles in the subregions of the transition region. Exactly one solid completely dissolves at $z = 0$, so the number of solids in the interval $(z_1, 0)$ is $P_1 + K_D - 1$. Eliminating the specific wave velocity v_{DU} from the flux balances, Eq. 45 yields $I - 1$ equations analogous to the coherence conditions of Eq. 41. In further analogy with Eq. 41, we expect that only $I - 2$ of the flux balances are linearly independent in the $P_1 + K_D - 1$ solid concentrations in the interval $(z_1, 0)$. We have already found that $P_1 + K_D - 1$ must equal $I - 2$ to determine J_1^+, so the flux balances determine the solid concentrations at $z = 0$.

This scheme of allocating solids applies to each succeeding upstream interval $(z_2, z_1), (z_3, z_2), \ldots, (z_\rho, z_{\rho-1})$. At each end point z_n one of the solids remaining from the original K_D downstream solids completely dissolves. At each end point as many of the P solids precipitate as possible without overconstraining the flowing phase concentrations at the end point. A solid precipitated in an intervening interval is present in each succeeding upstream interval. Thus the complete set of P precipitates will be present in the upstream interval $(-\infty, z_\rho)$. However, the flowing phase concentrations will not be overconstrained in the downstream constant state or any intervening intervals. Neither the DEC nor the PDEC apply to any of these intervening intervals because none are constant state regions.

The flowing phase concentrations at each interval end point z_n, $C_i|_{Zn}$, are independent of the actual value of z_n; they are fixed by the charge balance and the solid identities in the intervals (z_{n+1}, z_n) and (z_n, z_{n-1}) bounding z_n. Thus we may solve Eq. 47 for the position z_n in terms of b and the concentrations at z_n:

$$
bz_n = \ln\{[\nu_{si}^{(n)} C_i|_{Zn} - \alpha_s^{(n)}]/\beta_s^{(n)}\} \tag{48}
$$

The flux balances, the charge balance, the matching conditions at the z_n and the solid identities in each interval determine the constants $\alpha_s^{(n)}$ and $\beta_s^{(n)}$ independently of the value of the dissipation coefficient D_0. Equation 48 therefore implies that the product bz_n remains constant as the value of the coefficient D_0 varies. Now $N_{Pe} \propto 1/D_0$, so as dissipation approaches zero, N_{Pe} and $b = (1 - v_{DU})N_{Pe}$ become large positive numbers. Therefore z_n must decrease reciprocally to b. In other words, the length of each intervening interval in Figure 6 decreases as dissipation approaches zero. In this limit the multiple-discontinuity wave profile approaches the step change of the zero-dissipation solution.

Unlike the single-discontinuity wave, however, the upstream solids in U do not influence the flowing phase concentrations in D in the zero-dissipation limit. This is because the multiple-discontinuity wave profile does not converge uniformly to the constant upstream concentrations C_i^- on the interval $(-\infty, 0)$. Indeed

$$
\lim_{D_0 \to 0} \alpha_s^{(n)} + \beta_s^{(n)} \exp(bz) = \alpha_s^{(n)} \quad \text{for } z_n < z < z_{n-1}
$$

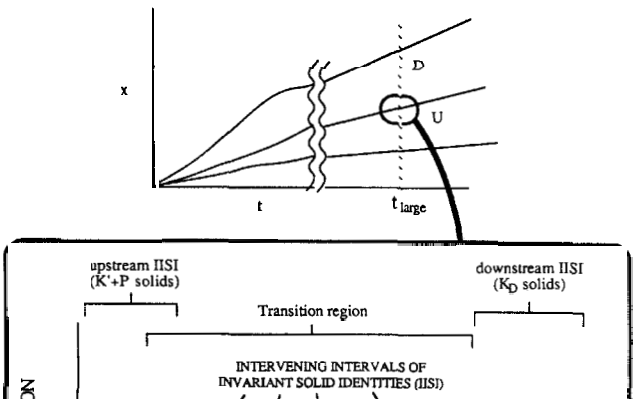

Figure 6. Shock structure of a precipitation/dissolution wave for $I \le K_D + P$ attains a constant pattern asymptotically.

One solid completely dissolves at each z_n $(n = 0, \ldots, \rho)$ producing discontinuities in the concentration derivatives that delimit ρ intervening IISI

but at the interval endpoints z_n

$$\lim_{D_o \to 0} \alpha_s^{(n)} + \beta_s^{(n)} \exp(bz_n) = \lim_{D_o \to 0} \nu_{si}^{(n)} C_i|_{Zn} = \nu_{si}^{(n)} C_i|_{Zn} \neq \alpha_s^{(n)}$$

The intervening intervals in the shock structure insulate the C_i^+ from the solubility products of the upstream precipitates. Only the solids in $(z_1, 0)$ influence the downstream concentrations via the PDEC. Numerical confirmation of the shock structure for an example of a multiple-discontinuity wave for $I \leq K_D + P$ appears in the Appendix.

Multiple-discontinuity waves when $\mathbf{I > K_D + P}$

Multiple-discontinuity waves can also exist when $I > K_D + P$. To discuss this class of waves, some terminology will be useful. Two solids S_1 and S_2 are "siblings" if at least one chemical species is present in both solids, i.e., if g_{i*1} and g_{i*2} are both positive for at least one independent species A_{i*}'. We define a "cousin" relationship recursively: two solids that have a common sibling are cousins, and two solids that have a common cousin are also cousins. A set of solids is a "family" if every solid in the set is a sibling or cousin of every other solid in the set. Thus the set of three binary solids denoted *AB*, *AC*, and *DC* constitutes a single family, because *AC* is a sibling of both *AB* and *DC*, making *AB* and *DC* cousins. However, the set of solids *AB* and *DC* is not a single family, because *AB* and *DC* are not siblings and cannot be cousins unless *AC* is present.

With these definitions we may divide the $K_D + P$ solids in regions *D* and *U* into families. If one or more of these families contains none of the K_D solids in *D* (i.e., if at least one family consists exclusively of solids that precipitate across the wave), then the shock structure of the wave must exhibit multiple discontinuities. In fact, if only a single discontinuity occurred, the DEC would force the wave to be noncoherent. To see this, note that by definition of a family the species composing the precipitate-only family are not present in any of the solids in region *D*. Thus exactly the same set of solubility products would influence the concentrations of these species both upstream and downstream of the wave. The reduced coherence equations involving this precipitate-only family would then imply that these species do not change concentration across the wave and that the wave velocity is zero.

However at least one family contains a solid that is present only in *D* because at least one solid must completely dissolve across every precipitation/dissolution wave. The species in that family therefore satisfy different sets of solubility products in regions *D* and *U*. Consequently the concentration changes in these species are generally nonzero across the wave, and the wave velocity for species in this family is positive. Thus the wave velocity for species in one family vanishes while the velocity for species in the second family is nonzero, violating the coherence condition Eq. 22. Consequently we must abandon the single-discontinuity profile and seek a more general form that preserves coherence.

The valid profile contains multiple discontinuities and is qualitatively identical to the profile for waves with $\rho > 0$, Figure 6. However, in this case the intervening IISI do not eliminate overconstraints, as when $\rho > 0$; rather they allow the coherence condition to be satisfied. To accomplish this, the intervening IISI contain siblings and/or cousins of the solids in the precipitate-only family. If I_F is the number of independent species in the precipitate-only family and K_F is the number of solids in the precipitate-only family, then there are $I_F - K_F$ reduced coherence equations for this family, like Eq. 24. Thus the intervening IISI $(z_1, 0)$ must contain K_F siblings/cousins of the precipitate-only family to provide sufficient jump conditions via the PDEC. Because no solid can precipitate in a precipitation/dissolution problem unless dissolution of another solid liberates species composing the precipitate, at least one of the solids in $(z_1, 0)$ must also be a sibling of a solid in *D*.

At least one of the solids in the interval $(z_1, 0)$ cannot be present in region *U*; otherwise the PDEC would be equivalent to the DEC. Since all intervening IISI shrink to zero width in the limit of zero-dissipation, the PDEC imposes the solubility product of a solid that is not present in region *D* or *U*, in contrast to the single-discontinuity wave for $I > K_D + P$ and the multiple-discontinuity wave for $I \leq K_D + P$. Numerical confirmation of an example of a multiple-discontinuity wave for $I > K_D + P$ appears in the Appendix.

The jump conditions for the three classes of precipitation/dissolution waves are summarized in Table 1.

Solving the general problem

We may now determine the flowing phase and solid concentrations in each sector of the proposed solution in the absence of dissipation, Figure 3. (This determination is only formal at this point because we have not yet discussed how to determine which solids are present in each sector.) The Γ_1 in sector R^J emanate from the $x = 0$ axis, carrying the injected composition throughout R^J, as in Figure 7. For Riemann conditions, R^J must therefore be a constant-state region. Similarly, the Γ_1 and Γ_2 carry the initial composition from the $t = 0$ axis throughout sector R^0, making R^0 a constant-state region. However, no flowing phase characteristics emanate from the $R^0 - R^1$ boundary, because that boundary is the unit slope salinity wave (Bryant, 1986). Thus J_1^1, the flowing phase invariant in R^1, does not influence J_1^0 in R^0.

Applying the reduced coherence conditions, the charge balance, and the DEC or the PDEC as needed, we determine J_1^n, $n = 1, \ldots, N$, in each sector R^n in terms of J_1^{n+1} in the immediately upstream sector R^{n+1}. The C_i in R^n are then calculated in terms of J_1^n and the solubility products for the solids in R^n. After determining the C_i in each sector, the concentration changes ΔC_i are known across every wave. The coherence conditions then determine J_2^n (i.e., the $C_k^{(n)}$, $k = 1, \ldots, K$) in each sector R^n in terms of the J_2^{n-1} in the immediately downstream sector R^{n-1} and the ΔC_i.

The Γ_1 in R^N carry J_1^N from the $R^N - R^J$ boundary throughout R^N. Since sector R^J is a constant state, the J_1^N must also be constant. Similarly, the J_1^n in each succeeding downstream sector $R^{N-1}, R^{N-2}, \ldots, R^1$, are constant. Since the solid concentrations do not change across a salinity wave, J_2^1 just upstream of the $R^1 - R^0$ boundary is identical to the constant J_2^0. The Γ_2 in R^1 carry the constant J_2 throughout R^1. Similarly the J_2^n in each upstream sector $R^2, \ldots, R^N$, R^J will be constant. Hence every sector is a constant-state region.

The coherence condition, Eq. 22, then implies that each wave velocity is constant, for the right side of Eq. 22 is constant across each wave. Hence the boundaries between sectors are straight lines emanating from the origin of the time-distance axes, Figure 7. Thus the solution to the precipitation/dissolution problem

Table 1. Classifying Precipitation/Dissolution Waves

No. of Discontinuities in Shock Structure	Degree of Overconstraint $\rho = K_D + P + 1 - I$	Jump Condition	Comments
Single	$\rho \leq 0$	DEC	Exactly one solid completely dissolves; all upstream solids have sibling or cousin downstream
Multiple	$\rho \leq 0$	PDEC	More than one solid completely dissolves; at least one upstream solid has no family member downstream; one or more solids appear in the shock structure that are not present either upstream or downstream
Multiple	$\rho > 0$	PDEC	$\rho + 1$ solids completely dissolve; ρ intervening IISI appear in shock structure

DEC, downstream equilibrium condition.
PDEC, partial downstream equilibrium condition.

under Riemann conditions in the absence of dissipation is self-similar and may be expressed in terms of a single independent variable $\xi = x/t$:

$$J_1(\xi) = J_1^n; J_2(\xi) = J_2^n \quad v_n < \xi < v_{n-1} \tag{49}$$

where superscript n indicates the constant state in sector R^n and v_n = specific wave velocity between sectors R^n and R^{n+1}.

The self-similarity and the presence of waves in the solution to the precipitation/dissolution problem are features common to other sets of hyperbolic conservation equations. But the form of the solubility product constraint introduces several interesting specifics that distinguish this solution from other theories.

1. All precipitation/dissolution waves are shocks; no spreading waves can occur in the precipitation/dissolution problem.
2. The coherence of precipiation/dissolution waves can be deduced.
3. The concentrations must be calculated in two passes. One must first determine the flowing phase concentrations in the downstream direction in every sector. Then and only then can one calculate the solid concentrations in each sector, proceeding in the upstream direction.

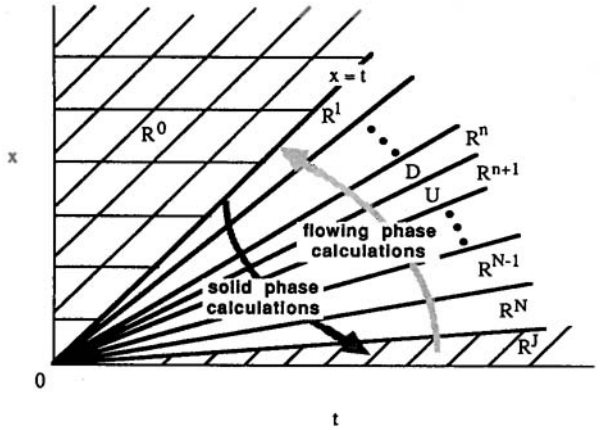

Figure 7. Solution to general precipitation/dissolution problem is a self-similar sequence of constant-state sectors.
Flowing phase characteristics carry injected conditions from time axis into sector R^J
Solid phase and flowing phase characteristics carry initial conditions from distance axis into sector R^0

Finding the Correct Sequence of Solid Identities

The solution described above expresses the flowing phase concentrations in terms of the solubility products of the solids in each sector R^n. To solve a particular problem, therefore, we must know the identities of the solids in each sector. The sequence of solid identities in sectors $R^1, R^2, \ldots, R^n$ we refer to as the solid sequence of the problem. To complete the solution we must relate the solid sequence to the initial and injected conditions and to the equilibria Eqs. 2 and 4.

For given boundary conditions and equilibria, many different potentially valid solid sequences can be written (Bryant, 1986). The solid identities in each sequence uniquely determine the flowing phase and solid concentrations in the sectors of the wave solution Eq. 49. However, since we assume a unique solution, only one of these sequences can be correct, i.e., physically valid. Several features distinguish the physically valid solid sequence.

1. The waves in the valid sequence are ordered.
That is, the velocity of any wave exceeds the velocity of every wave upstream.
2. The calculated concentrations satisfy local equilibrium.
This condition can be violated by incorrect sequences because the coherence conditions and the jump conditions involve only the solids in the sequence and in the shock structures. Thus the flowing phase concentrations calculated for a particular region may exceed the solubility products of solids not present in that region of the sequence.
3. All calculated concentrations and velocities must be non-negative.
4. Any multiple discontinuity waves that occur in the solid sequence impose certain constraints related to the dissipation structure of the waves (Bryant, 1986).

Under our assumption of uniqueness only one of the potentially valid solid sequences for a given problem will satisfy all of these criteria. Solution of the precipitation/dissolution problem thus becomes a search for the correct solid sequence. This search is analogous to the solution of chromatography problems along characteristics in hodograph space (Rhee et al., 1970; Helffer-

ich and Klein, 1970). However, because of the two directions involved in the calculation of flowing phase and solid concentrations, the one-directional solution scheme for chromatography problems does not extend to precipitation/dissolution problems. Instead we use the criteria for physical validity to derive "solution functions" for classes of precipitation/dissolution problems (Bryant, 1986). (Precipitation/dissolution problems that are subject to the same set of solubility product constraints comprise a single "class.")

The criteria for physical validity can be expressed in terms of the solubility products for that class of problems, the initial conditions and the injected conditions. Thus expressed, the criteria define the range of boundary conditions and solubility products over which the various sequences give the correct solution. Thus a solution function maps a class of possible precipitation/dissolution problems to a space of solid sequences. Once the solution function has been derived, the correct solid sequence for any problem in the class is readily obtained.

An example of the solution function

To illustrate the solution function, consider the class of precipitation/dissolution problems subject to the solubility product constraints of two binary solids, AB and AC. If only solid AB is initially present in a permeable medium, two solid sequences are possible:

Sequence 1 I-$\{AB\}$-J

Sequence 2 I-$\{AB\}$-$\{AC\}$-J

where I and J represent the initial and injected conditions, respectively. When J is undersaturated fluid the first sequence corresponds to the dissolution of solid AB from the medium; the second corresponds to the simultaneous precipitation of solid AC and dissolution of solid AB, followed by the dissolution of AC. States I, $\{AB\}$, $\{AC\}$, and J correspond to sectors R^0, R^1, R^2, and R^J, respectively, in Figure 7; see Table 2.

Four other solid sequences are possible in this class of problems. If only solid AC is initially present, then the possible solid sequences are I-$\{AC\}$-J and I-$\{AC\}$-$\{AB\}$-J. If both solids AB and AC are initially present, there are again two possible solid sequences: I-$\{AB, AC\}$-$\{AB\}$-J and I-$\{AB, AC\}$-$\{AC\}$-J.

We derive the solution function for a subclass of this class of problems, the set of problems in which solid AB is initially present and for which the injected fluid contains no species A or B. The injected conditions are undersaturated with respect to both solids. The concentrations and wave velocities for the two solid sequences possible in this subclass appear in Table 2.

Criteria of Validity for Sequence 1. The wave velocities are always ordered in sequence 1, because the AB-dissolution wave between sectors R^1 and R^J necessarily travels slower than the salinity wave between sectors R^0 and R^1. Since AC is not present in sector R^1 in sequence 1, the calculated concentrations of A and C in R^1 may exceed the solubility product of AC. Thus the criteria for physical validity for sequence 1 reduce to local equilibrium in sector R^1: $C_A^I C_C^I \le K_{AC}$, where superscript I refers to sector R^1. Substituting from Table 2 for C_A^I and C_C^I yields

$$C_C^J \le K_{AC}/K_{AB}^{1/2} \tag{50}$$

Criteria of Validity for Sequence 2. In sequence 2, the wave velocities are ordered if $v_1 > v_2$. According to Table 2, this condition is equivalent to $C_{AB}^0/C_B^I < C_{AC}^{II}/C_A^{II}$. Substitution from Table 2 for these values and simplification yields: $K_{AB}^{1/2} C_C^J > K_{AC}$.

Table 2. Concentrations and Velocities for Solid Sequences in a Subclass of Two-solid Precipitation/Dissolution Problems

Sequence 1: I-$\{AB\}$-J

Species	Region R^0	R^1	R^J
A	C_A^0	$K_{AB}^{1/2}$	$C_A^J (=0)$
B	C_B^0	$K_{AB}^{1/2}$	$C_B^J (=0)$
C	C_C^0	C_C^J	C_C^J
AB	$\underline{C}_{AB}^0$	$\underline{C}_{AB}^0$	—
AC	0	0	—

$v_0 = 1$; $v_1 = (1 + \underline{C}_{AB}^0/K_{AB}^{1/2})^{-1}$

Sequence 2: I-$\{AB\}$-$\{AC\}$-J

Species	Region R^0	R^1	R^2	R^J
A	C_A^0	C_A^I	C_A^{II}	$C_A^J (=0)$
B	C_B^0	K_{AB}/C_A^I	$C_B^J (=0)$	$C_B^J (=0)$
C	C_C^0	K_{AC}/C_A^I	K_{AC}/C_A^{II}	C_C^J
AB	$\underline{C}_{AB}^0$	$\underline{C}_{AB}^0$	0	—
AC	0	0	$\underline{C}_{AC}^{II}$	—

$v_0 = 1$; $v_1 = (1 + \underline{C}_{AB}^0/C_B^I)^{-1}$; $v_2 = (1 + \underline{C}_{AC}^{II}/C_A^{II})^{-1}$

where $C_A^I = \{-C_C^J + [(C_C^J)^2 + 4K_{AB} + 4K_{AC}]^{1/2}\}/2$

$C_A^{II} = \{-C_C^J + [(C_C^J)^2 + 4K_{AC}]^{1/2}\}/2$

$\underline{C}_{AC}^{II} = \underline{C}_{AB}^0 (C_C^{II} - C_C^I)/C_B^I$

In sequence 2 solid AB is not present in sector R^2, and solid AC is not present in sector R^1. But since $C_B^{II} = 0$, the concentrations in sector R^2 are undersaturated with respect to AB. The DEC forces the concentrations in sector R^1 to be saturated with respect to AC. Hence local equilibrium is satisfied in both sectors, and the criteria for physical validity for sequence 2 reduce to the wave-ordering criterion:

$$C_C^J > K_{AC}/K_{AB}^{1/2} \tag{51}$$

The solution function for this subclass of problems maps all problems in the subclass with injected conditions and solubility products that satisfy Eq. 51 to sequence 2, I-$\{AB\}$-$\{AC\}$-J. It maps all problems in the subclass that satisfy Eq. 50 to sequence 1, I-$\{AB\}$-J. Since Eqs. 50 and 51 are complementary, no problem in the subclass can satisfy the criteria of physical validity for both sequences. Hence each problem in this subclass has a unique solution. Furthermore, any sequence in the subclass satisfies either Eq. 50 or Eq. 51, so the solution function is exhaustive for this subclass.

Similar analysis for general injected conditions and for the four other possible sequences generates the solution function for the entire class of AB, AC-precipitation/dissolution problems.

Conclusions

We have obtained the general analytical solution for one-dimensional flow through permeable media with precipitation/dissolution reactions at equilibrium under Riemann boundary conditions. The solution is self-similar, exhibiting constant-state

sectors emanating from the origin of the time-distance axes. Coherent shocks separate the sectors. Each shock (except for the salinity wave) completely dissolves at least one solid; the exact number of solids dissolved equals the number of discontinuities in the shock structure. Concentrations in adjacent sectors are related by mass balances (coherence conditions) across the wave separating the sectors. If solids precipitate across a wave, jump conditions are required in addition to the mass balances. The structure of the waves in the presence of dissipation provides these jump conditions. The downstream equilibrium condition is the jump condition when the structure exhibits a single discontinuity. A partial downstream equilibrium condition applies when multiple discontinuities occur in the structure. The coherence conditions and jump conditions determine the problem in terms of the identities of the solids in the constant-state sectors. Thus solving the precipitation/dissolution problem is equivalent to finding the correct solid sequence for the given boundary conditions. The criteria of physical validity determine the correct solid sequence.

Acknowledgment

The Stimulation, Logging and Formation Damage Research Program at the University of Texas supported this work. Contributors to the program include Amoco Production, Arco Oil and Gas, BASF Wyandotte, British Petroleum International, Chevron Oil Field Research, Cities Service Technology Center, Conoco, Exxon Chemical, Exxon Production Research, Japan National Oil, Kerr-McGee, Marathon Oil, Minnesota Mining 3M Center, Norsk Hydro Research, Phillips Petroleum, Shell Development, Smith Energy Services, Sun Exploration and Production, Tenneco Exploration and Production, Texaco Bellaire Research Center, Titan Services, and Union Oil of California.

Notation

A_r = dependent flowing phase species r
A_i' = independent species i
C_i' = concentration of independent species A_i', mol/unit pore volume
C_r = concentration of dependent species A_r, mol/unit pore volume
C_j = concentration of flowing phase species j, mol/unit pore volume
C_i = total concentration of independent species A_i' in flowing phase as a function of position and time, given by $h_{ij}C_j$, mol/unit pore volume
C_i^T = total concentration of independent species A_i' in both flowing and solid phases, given by $C_i + g_{ik}\underline{C}_k$, mol/unit pore volume
$\underline{C}_k$ = concentration of solid S_k, mol/unit pore volume
C = column vector $(C_1, C_2, \ldots, C_I)$ of total flowing phase concentrations
$\underline{C}$ = column vector $(\underline{C}_1, \underline{C}_2, \ldots, \underline{C}_K)$ of solid concentrations
D = sector of invariant solid identities downstream of arbitrary boundary in solution to precipitation/dissolution problem
D_0 = coefficient of dissipation (diffusion or dispersion), L^2/t
F_j = dissipative flux of species j, mol/unit pore volume
g_{ik} = number of molecules of independent species A_i' in a molecule of solid S_k
$[g_{ik}]$ = $I \times K$ matrix of stoichiometric coefficients g_{ik}
h_{ij} = number of molecules of independent species A_i' in flowing phase species j
I = number of elements in a precipitation/dissolution problem or in a wave; initial conditions
IISI = interval(s) of invariant solid identities
J = number of chemical species in flowing phase; injected conditions
J_1 = flowing phase Riemann invariant
J_2 = solid phase Riemann invariant
K_k^{sp} = solubility product of solid S_k
K_r = equilibrium constant for formation reaction of A_r
K = number of possible soluble solids in a precipitation/dissolution problem
K' = number of solids present in both sectors upstream and downstream of arbitrary wave
K_D = number of solids present in sector downstream of arbitrary were
K_R = number of solids present in an arbitrary region R of invariant solid identities
K_z = number of solids present in an IISI moving with a wave
L = characteristic length of a permeable medium
L_1 = differential operator $\partial/\partial_t + \partial/\partial_x$
L_2 = differential operator $-\partial/\partial_t$
L_3 = differential operator $(1 - v)d/dz - (N_{P_e})^{-1} d^2/dz^2$
N_{P_e} = Peclet number, given by $uL/D_0\phi$
P = number of solids that precipitate across arbitrary wave
P_1 = number of solids that precipitate in IISI immediately upstream of sector D in shock structure of wave for $I \le K_D + P$
RISI = region(s) of invariant solid identities
R^n = RISI in solution to the Riemann problem
S_k = soluble solid k
t = time (normalized by $L\phi/u$)
t_{large} = time at which constant-pattern wave profile is established
U = RISI upstream of arbitrary boundary in solution to precipitation/dissolution problem
u = superficial fluid velocity, L/t
v = wave velocity (or slope of a boundary between regions of invariant solid identities) as a fraction of superficial fluid velocity
v_{DU} = slope of arbitrary boundary in solution to precipitation/dissolution problem
v_n = velocity of wave between sectors R^n and R^{n+1} in solution to precipitation/dissolution problem
w_j = charge of species j
x = position in permeable medium (normalized by length L)
x_{DU} = arbitrary boundary between RISI in solution to precipitation/dissolution problem
X_s = component of flowing phase invariant
z_n = position of end point of intervening IISI in shock structure
z = dimensionless reference frame moving with wave velocity v_{DU}

Greek letters

α = parameter in family of flowing phase characteristics
α_{ir} = number of molecules of independent species A_i' in a molecule of dependent species A_r
α_s = constant of integration in flowing phase concentration profile in shock structure
β = parameter in family of solid phase characteristics
β_s = constant of integration in flowing phase concentration profile in shock structure

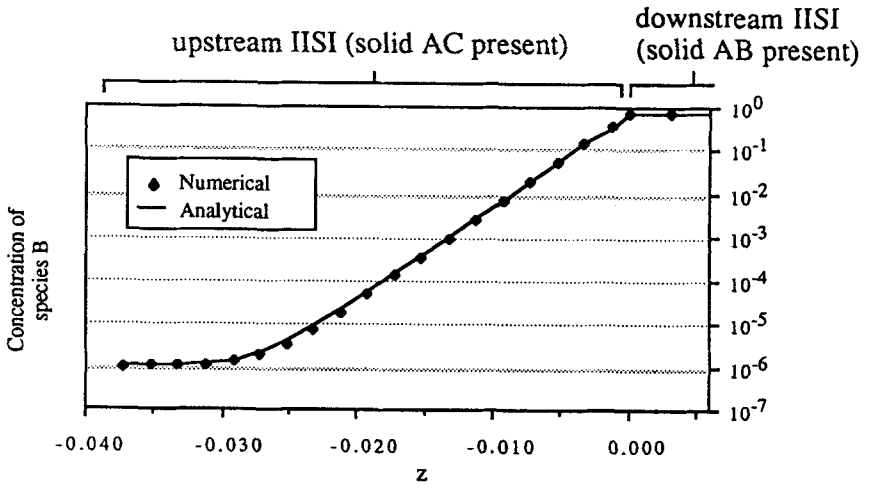

Figure 8. Numerical confirmation of concentration profile of species *B* in shock structure of an *AC*-precipitation/*AB*-dissolution wave.

A single discontinuity occurs at $z = 0$. Semilog plot emphasizes exponential dependence on distance z in transition region, $-0.30 < z < 0.0$.

γ_k = constant of integration in solid concentrations profile in shock structure
ν_{si} = stoichiometric coefficient defining the moles of element s in species i
Γ_1 = family of flowing phase characteristics
Γ_2 = family of solid phase characteristics
δ_{ij} = Kronecker delta
∂R = boundary of region R
ϕ = porosity of medium
ρ = degree of overconstraint if DEC were to apply when $I \leq K_D + P$, given by $K_D + P + 1 - I$
ξ = self-similarity parameter given by x/t

Subscripts and superscripts

inj = injected conditions
init = initial conditions
+ = downstream of boundary
− = upstream of boundary
(n) = value in intervening IISI in shock structure
I, II, . . . , N; 1, 2, . . . N = value in sector R^1, R^2, . . . , in solution to precipitation/dissolution problem
0, J = value in initial conditions sector R^0 and injected conditions sector R^J, respectively

Appendix: Examples of Precipitation/Dissolution Waves and Their Shock Structures

In this section we present examples of each of the three types of precipitation/dissolution waves, Table 1. We also confirm the analytical solution for the shock structure of these waves numerically. To do so, we modify a finite-difference computer model for the general reactive flow problem to account explicitly for dissipation (Bryant, 1986). Since the model solves the original Riemann problem in $x - t$ space, Eqs. 2, 5, 6, and 11, the

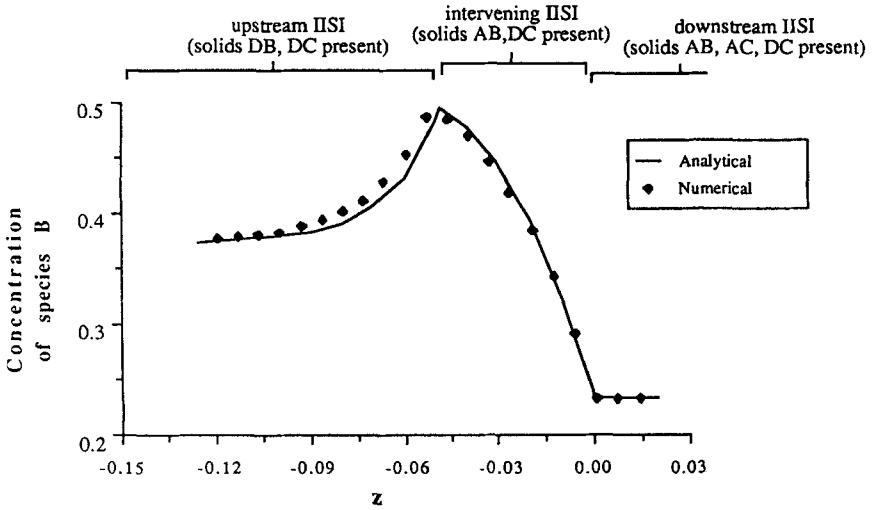

Figure 9. Numerical confirmation of concentration profile of species *B* in shock structure of a *DB*-precipitation/*AB*, *AC*-dissolution wave.

Two discontinuities occur, at $z = 0$ and $z = 0.047$
Concentration of B is constant for $z > 0$ and $z < -0.13$

numerical solution provides an independent check on the assumptions used to derive the shock structures.

A single-discontinuity wave

Consider an AC-precipitation/AB-dissolution wave such as the one between sectors R^1 and R^2 in sequence 2 of Table 2. There are three elements (A, B, and C), one dissolving solid (AB), and one precipitate (AC), so $I = 3, K_D = 1, K' = 0, P = 1$, and $\rho = 0$. Since AB and AC are siblings, this is a single-discontinuity wave. For ease of comparison with the numerical model, assign the values $K_{AB} = 1$; $K_{AC} = 1$; $N_{P_e}^{-1} = 0.001167$, $C_A^J = C_C^J = 0.9$, and $C_B^J = 1.0 \times 10^{-6}$. The flowing phase invariant upstream of this wave has components

$$X_1 = C_A - C_C$$
$$X_2 = C_B$$

Thus $C_B = \alpha_2 + \beta_2 \exp(bz)$. Evaluation of the integration constants and wave velocity yields

$$C_B = C_B^{II} + (C_B^I - C_B^{II}) \exp(bz)$$
$$= 10^{-6} + 0.707 \exp(502z)$$

This relation is plotted as the solid curve in Figure 8.

The numerical solution for the concentration profile of species B at time $t = 0.202$ was translated to a z axis moving with the wave; it comprises the data points in Figure 8. The agreement in Figure 8 confirms the validity of the constant-pattern analysis in the moving reference frame, Eqs. 26–36.

A multiple-discontinuity wave ($I \leq K_D + P$)

Suppose solids AB, AC, and DC are initially present in a medium at concentrations $\underline{C}_{AB} = 0.40$, $\underline{C}_{AC} = 1.40$, and $\underline{C}_{DC} = 2.08$, and we inject a fluid with concentrations $C_A = C_C = 10^{-7}$ and $C_B = C_D = 0.25$. For solubility product constraints $K_{AB} = 0.302$, $K_{AC} = 1.9953$, $K_{DC} = 0.7413$, and $K_{DB} = 0.3981$, the correct solid sequence is I-$\{AB, AC, DC\}$-$\{DC, DB\}$-$\{DB\}$-J. For the wave between constant states $\{AB, AC, DC\}$ and $\{DC, DB\}$, we have $I = 4$, $K_D = 3$, $K' = 1$, $P = 1$, and $\rho = 1$. Thus the shock structure of this wave must exhibit $\rho + 1 = 2$ discontinuities. The IISI intervening between the upstream and downstream constant states contains solids AB and DC. We compare the analytical solution ($N_{P_e}^{-1} = 0.0107$) for the concentration profile of species B in the shock structure with the numerical solution in Figure 9. Again the agreement confirms the constant-pattern analysis.

A multiple-discontinuity wave ($I > K_D + P$)

Suppose solid AB is initially present in a medium at concentration $\underline{C}_{AB} = 1.0$, and we inject a fluid with concentrations $C_A = 0.6843$, $C_B = 0.4214$, $C_C = 0.4283$, and $C_D = 0.5270$. For solubility product constraints $K_{AB} = 3.39$, $K_{AC} = 0.603$, and $K_{DC} = 0.240$, the correct solid sequence is I-$\{AB\}$-$\{DC\}$-J. For the wave between constant states $\{AB\}$ and $\{DC\}$, we have $I = 4$, $K_D = 1$, $K' = 0$, $P = 1$, and $\rho = -1$. Since AB and DC are not siblings, this must be a multiple-discontinuity wave; solid DC constitutes a family that contains only precipitates. In this case the shock structure exhibits an IISI intervening between the upstream and downstream constant states that contains solid AC, a sibling of both AB and DC. We compare the analytical solution ($N_{P_e}^{-1} = 0.00167$) for the concentration profile of species C in the shock structure with the numerical solution in Figure 10. Again the agreement confirms the constant-pattern analysis.

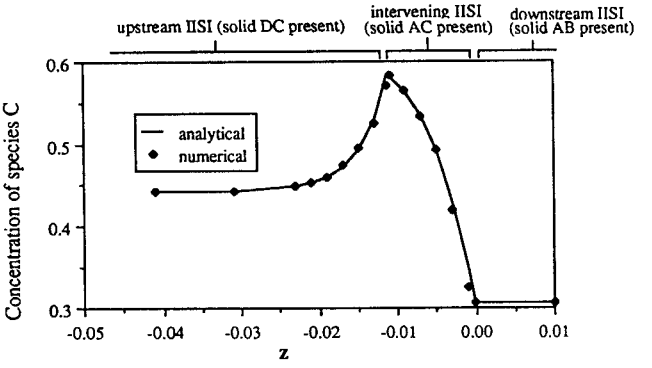

Figure 10. Numerical confirmation of concentration profile of species C in shock structure of a DC-precipitation/AB-dissolution wave.
Two discontinuities occur, at $z = 0$ and $z = -0.011$

The PDEC means that the flowing phase concentrations downstream of this wave will satisfy the solubility product of AC, even though AC is not present in the absence of dissipation. The intervening interval containing AC does not become a constant-state region, for then the solid sequence would be I-$\{AB\}$-$\{AC\}$-$\{DC\}$-J. For the given boundary conditions, the velocity of the AB-dissolution/AC-precipitation wave is less than the velocity of the AC-dissolution/DC-precipitation wave. Thus the sequence I-$\{AB\}$-$\{AC\}$-$\{DC\}$-J cannot be physically valid.

Literature cited

Bryant, S. L., "Wave Behavior in Reactive Flow Through Permeable Media," Ph.D. Diss. Univ. Texas, Austin (1986).

Bryant, S. L., R. S. Schechter, and L. W. Lake, "Interactions of Precipitation/Dissolution Waves and Ion Exchange in Flow Through Permeable Media," *AIChE J.*, (**32**, 5, 751, 1986).

Courant, R., and K. Friedrichs, *Supersonic Flow and Shock Waves*, Interscience, New York, 79–171 (1948).

Cussler, E. L., J. Kopinsky, and J. A. Weimer, "The Effect of Pore Diffusion on the Dissolution of Porous Mixtures," *Chem. Eng. Sci.* **38**(12), 2027 (1983).

DeVault, D., "The Theory of Chromatography," *J. Am. Chem. Soc.* (Apr., 1943).

Fogler, H. S., and S. D. Rege, "Porous Dissolution Reactors," *Chem. Eng. Commun.*, **42**, 291 (1986).

Glueckauf, E., "Contributions to the Theory of Chromatography," *Proc. Roy. Soc. Lond.*, **A 186**, 35 (1946).

Helfferich, F., and G. Klein, *Multicomponent Chromatography*, Dekker, 1–225 (1970).

Lake, L. W., and F. Helfferich, "Cation Exchange in Chemical Flooding. 2: The Effect of Dispersion, Cation Exchange, and Polymer/Surfactant Adsorption on Chemical Flood Environment," *Soc. Pet. Eng. J.*, (Dec., 1978).

Lax, P., "Hyperbolic Systems of Conservation Laws. II," *Comm. Pure Appl. Math.* (Nov., 1957).

Lighthill, J., *Waves in Fluids*, Cambridge, 89–199 (1978).

Rhee, H.-K., R. Aris, and N. Amundson, "Theory of Multicomponent Chromatography," *Phil. Trans. Roy. Soc. Lond.*, **A 267**, 419 (1970).

Smith, W., and R. Missen, *Chemical Reaction Equilibrium Analysis: Theory and Algorithms*, Wiley, New York, 14–36 (1982).

Stohs, M., "A Study of Metal Ion Migration in Soils from Drilling Mud Pit Discharges," M. S. Thesis, Univ. Texas, Austin (1986).

Taniuti, T., and K. Nishihara, *Nonlinear Waves*, Pitman, 1–99 (1983).

Tondeur, D., and G. Klein, "Multicomponent Ion Exchange in Fixed Beds," *Ind. Eng. Chem. Fundam.* **6,** 351 (1967).
Walsh, M., "Geochemical Flow Modeling," Ph.D. Diss., Univ. Texas, Austin (1983).
Walsh, M., S. Bryant, R. Schechter, and L. Lake, "Precipitation and Dissolution of Solids Attending Flow Through Porous Media," *AIChE J.*, (**30,** 3, 317 1984).
Whitham, G., *Linear and Nonlinear Waves,* Wiley, pp. 1–67, 1974.
Wilson, J., "A Theory of Chromatography," *J. Am. Chem. Soc.,* **62,** 1583 (1940).

Manuscript received Sept. 5, 1986, and revision received Jan. 27, 1987.